Indian Journal of Chemical Technology
Vol. 24, January 2017, pp. 73-81

Removal of Direct Red 12B from aqueous medium by $ZnCl_2$ activated *Jatropha* husk carbon: Adsorption dynamics and equilibrium studies

Kumaravel Karthick*, Chinnaya Namasivayam & Lingassamy Arul Pragasan
Environmental Chemistry Division, Department of Environmental Sciences, Bharathiar University, Coimbatore 641 046, India
E-mail: karthik.envchem@gmail.com

Received 31 July 2014; accepted 13 September 2015

Adsorption isotherms and kinetics of adsorption of Direct Red 12B (DR 12B) on zinc chloride activated carbon prepared from Jatropha husk (ZAJHC) have been determined from batch tests. Effects of contact time, initial dye concentration, initial *p*H, adsorbent dose and solution temperature have been investigated. The equilibrium data are best represented by Langmuir isotherm model, showing monolayer adsorption capacity (Q_o) of 39 mg g^{-1}. The kinetic data are fitted to pseudo-first-order, pseudo-second-order and intraparticle diffusion models, and are found to follow closely the pseudo-first-order kinetic model. Thermodynamic parameters such as standard enthalpy (ΔH^o), standard entropy (ΔS^o) and standard free energy (ΔG^o) have been evaluated. The adsorption interaction is found to be endothermic in nature. Acidic *p*H is favourable for the adsorption of DR 12B. Desorption studies show that chemisorption seems to be the major mode of adsorption. ZAJHC is shown to be a promising adsorbent for removal of DR 12B from aqueous solutions.

Keywords: Adsorption, Direct Red dye, Isotherms, Jatropha husk carbon, Kinetics

Environmental pollution increases with increasing industrial developments. The textile industry plays a part in the economy of several countries around the world. Dyeing is a fundamental operation during textile fiber processing. This operation causes the production of coloured wastewaters, depending on the degree of fixation of the dyestuffs on the substrates, which varies with the nature of the substances, the desired intensity of coloration, and the application method[1]. Textile companies, dye manufacturing industries, paper and pulp mills, tanneries, electroplating factories, distilleries, food companies and a host of other industries discharge coloured wastewaters[2].

Dyes are organic compounds with a complex aromatic molecular structure that can bring bright and firm colour to other substances. However, the complex aromatic molecular structures of dyes make them more stable and more difficult to biodegrade[3]. Azo groups are the most common chromophore in acid, direct and dispersive dyes and are also frequently used as components in reactive dyes[4]. About a half of global production of synthetic textile dyes is classified into azo compounds that have the chromospheres of –N=N– unit in their molecular structure. Azo dyes are very difficult to be treated in environmental systems, because the sulfonic acid groups in their structures make the dyes water-soluble and polar[5]. Synthetic dye residues affect photosynthetic activity by preventing light penetration in aquatic life and produce toxic chemicals which have a detrimental effect on flora, fauna and human beings. Most synthetic dyes are carcinogenic, highly toxic in nature and create problems in life system and cause allergic dermatitis, skin irritation and mutation to humans[6,7].

There are many processes available for the removal of dyes by conventional treatment technologies including biological and chemical oxidation, foam flotation, biodegradation, advanced oxidation, photocatalysis, flocculation, coagulation, precipitation, fungal decolorization, membrane filtration, electrochemical techniques, ozonation and adsorption[8]. Among these techniques adsorption has been proved to be an excellent way to treat dye effluents, offering advantages over conventional processes. Also, adsorption provides an attractive alternative treatment, especially if the adsorbent is inexpensive and readily available[9].

In developing countries like India, industries cannot afford to use conventional wastewater treatment chemicals like alum, ferric chloride, polymer flocculants and coal based activated carbon because they are not cost-effective. An inexpensive and more easily available adsorbent would make the removal of pollutants an economically viable alternative[10]. Activated carbon is widely used as an adsorbent for many species because of its high efficiency. However because of the cost involved a search for alternative adsorbents that could provide an economical solution is very important in developing countries like India[11].

Many studies have been made using different source materials for ACs like, coir pith, peanut hull, sawdust, rice hull, paddy straw, oil palm shell, pistachio-nut shells, sunflower seed hull, cashew nut shell, pomegranate peel, Indian rosewood, maize waste, mango seed kernel, coconut waste, avocado kernel, fenugreek mucilage and various blends of these. However search for cost-effective, efficient adsorbent is continuing[12,13].

Jatropha husk (JH) is generated in large quantities as an agro-industrial solid waste in the bio diesel production industries. JH constitutes nearly 80% of the dried vegetable. Activation of JH with $ZnCl_2$ generates more micro porosity and surface area which leads to an increase in the adsorption capacity[14]. When a lignocellulosic precursor is activated with increasing concentrations of zinc chloride, phosphoric acid and potassium hydroxide there is a strong development of porosity, initially centered in the microporosity[15]. The adsorption capacity increased on ZAJHC with increase in surface area and porosity when compared to thermal activated *Jatropha* husk carbon[16]. The objective of this present study was to explore the feasibility of using ZAJHC as an adsorbent for the removal of DR 12B from water. This dye is widely used in dyeing industries of Coimbatore and Tiruppur, Tamil Nadu, India.

Experimental Section

Adsorbent

ZAJHC was prepared as reported in literature[12]. Characteristics of ZAJHC are shown in Table 1.

Table 1 — Characteristics of ZAJHC

S. No	Characteristics	Value
1	$p\text{H}_{\text{ZPC}}$	6.8
2	Specific gravity	1.03
3	Bulk density (g L^{-1})	0.20
4	Porosity (%)	81
5	S_{BET} (m^2 g^{-1})	822
6	Ion exchange capacity (meq g^{-1})	Nil
7	Iodine number (mg g^{-1})	91

DR 12B was procured from BDH/Loba, Mumbai, India and used as such without further purification. All the other chemicals used were of AR grade. A stock solution of 1000 mg L^{-1} of DR 12B was prepared by dissolving the dye in double distilled water. Solutions of various concentrations were prepared by using the above solution. The solutions were stored in brown glass bottles to avoid degradation in light. Absorbance measurements were carried out for DR 12B using UV-Vis spectrophotometer (Specord 200, Analytic Jena, Germany). The absorption maximum at 508 nm for DR 12B was used as the monitoring wavelength for the measurement of absorbance. Calibration graphs were made for DR 12B and the concentrations were estimated using calibration graphs.

Structure of DR 12B

DR 12B has two azo, di-sulfonic acid groups and contains amine group. The solubility of dye depends on the number of sulphonic groups ($-SO_3Na$) present in the dye molecule. The diazenyl group is responsible for the formation of covalent bonds between the dye and the adsorbent[17]. The rate of adsorption may be lowered by the dye's structural complexity that is inversely proportional to the number of sulfonate group present[18] (Fig. 1).

DR 12B is also known as direct red 31. Its IUPAC name is 7,7'-iminobis(4-hydroxy-3-(2-phenyl diazenyl)-2-naphthalenesulfonic acid sodium salt (molecular formula $C_{32}H_{21}N_5Na_2O_8S_2$ and molecular weight 713.65) and belongs to the class of azo dyes.

Instrumental analysis of ZAJHC

The surface morphology of unloaded and loaded ZAJHC was examined using scanning electron microscope (SEM-JSM, 840A, JEOL, Japan). After adsorption, DR 12B loaded ZAJHC carbon samples were filtered using a suction pump on qualitative filter paper and stored in a vacuum desiccator, which was later used for instrumental analysis.

Batch adsorption experiments

Adsorption experiments were carried out for DR 12B to investigate effects of various parameters such as initial concentration of adsorbate, contact time,

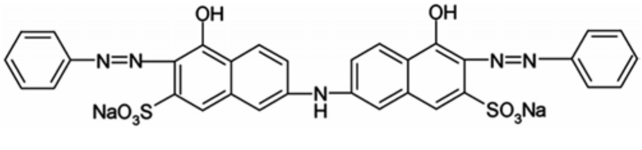

Fig. 1 — Structure of DR 12B.

adsorbent dose, initial *p*H and temperature. Solutions containing desired concentrations of DR 12B at *p*H 2.0 and ZAJHC were placed in 100 mL conical flasks and agitated at 200 rpm, 35°C on a Wise Cube shaking incubator (DAIHAN Scientific, Co., Ltd. Korea). After the predetermined time intervals, the samples were withdrawn and the supernatant was separated from the ZAJHC by centrifugation at 2500 rpm for 30 min. Then the concentration of the residual dye was determined as said earlier. Effect of *p*H was studied in the *p*H range 2.0-10.0 by adjusting the *p*H of solutions using 1 M HCl and 1 M NaOH solutions by means of a *p*H meter (Elico, Mode LI-107, Hyderabad, India). Effect of temperature was studied at different temperatures such as 313 K, 323 K and 333 K on 30 mg L^{-1} DR 12B solution.

Desorption studies

The adsorbent that was used for adsorption of 20 mg L^{-1} of dye solution was separated from the dye solution by centrifugation. The dye-loaded adsorbent was separated using Whatman filter paper and washed gently with water to remove any unadsorbed dye. Several such samples were prepared. Then the spent adsorbent was agitated with 50 mL of distilled water, adjusted to different *p*H values for equilibrium time. The desorbed dye was estimated as before.

Results and Discussion

SEM observations

High surface area and pore structure are the basic parameters for an effective adsorbent. When the porosity increases the surface area also increases. ZAJHC shows tremendous, perfect and constructed pore structures on the surface. Higher volume of pores developed from the $ZnCl_2$ activation acts as a route for the contaminants to enter into the micro pores presented in Fig. 2(a). After adsorption, the surface of ZAJHC was loaded with DR 12B shown in Fig. 2(b). Waxy substance coating on the surface of the ZAJHC clearly shows that the dyes were strongly adsorbed on ZAJHC.

Effect of *p*H on adsorption of DR 12B onto ZAJHC

Experiments were carried at different *p*H values varying from 2.0-10.0. The results show that the removal of DR 12B is higher in acidic *p*H (*p*H = 2.0) presented in Fig. 3(a). Solution *p*H would affect both aqueous chemistry and surface binding-sites of the adsorbents[19]. The hydrogen ion and hydroxyl ions are adsorbed quite strongly and therefore adsorption of other ions is affected by the *p*H of the solution. Change of *p*H affects adsorptive process through dissociation of functional groups on the adsorbent surface active sites. Anionic dyes are known to ionize to a high degree in aqueous solutions to form coloured anions due to the sulfonated groups in their structures. The two $-SO_3-$ groups of DR 12B are easily dissociated and have negative charges in the aquatic environment[20]. The higher uptakes obtained at very acidic *p*H can be attributed to the electrostatic interaction between the positively charged ZAJHC [pH_{zpc}, 6.8] and the acid (anionic) dyes. When the *p*H of the system was increased, the number of negatively

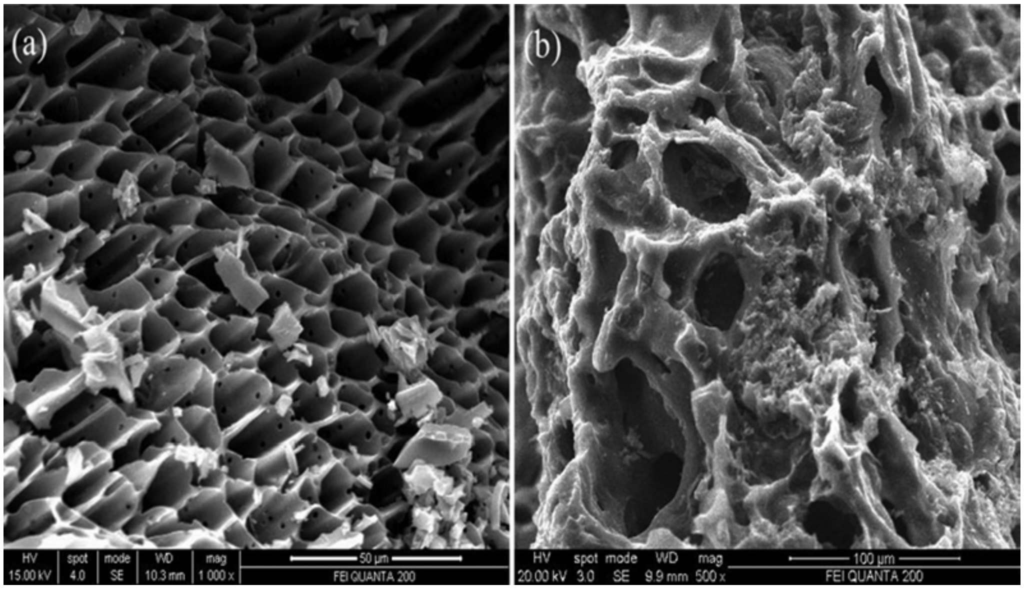

Fig. 2 — SEM images for (a) ZAJHC and (b) ZAJHC after adsorption of DR 12B.

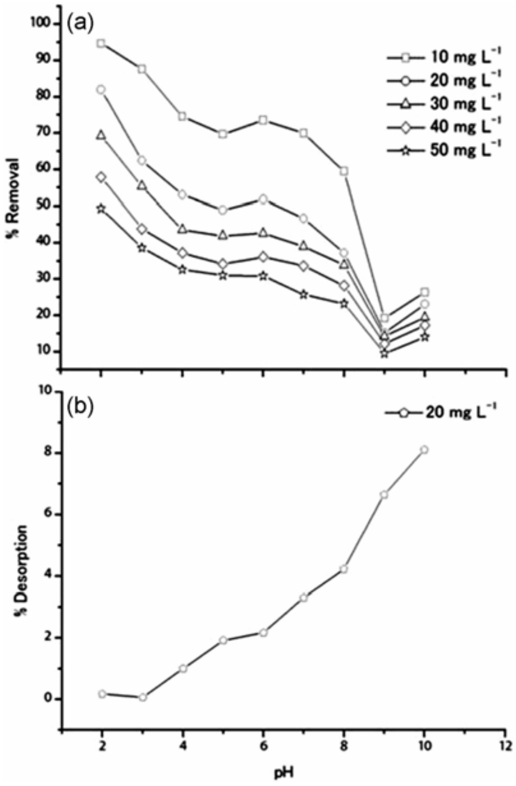

Fig. 3 — Effect of initial *p*H on adsorption (a) and desorption (b) of DR 12B onto ZAJHC.

charged site increases and the number of positively charged site decreases. A negatively charged surface site on the ZAJHC does not favour the adsorption of dye anions due to the electrostatic repulsion. Also, lower adsorption of acid dyes at alkaline *p*H is due to the presence of excess hydroxyl ions competing with the dye anions for the adsorption sites[21].

Desorption studies

Desorption studies as a function of *p*H were conducted to analyze the possibility of reuse of the adsorbent for further adsorption and to make the process more economical[22]. Figure 3(b) shows the per cent desorption were < 16.0 in the *p*H range 2.0-10.0 for the dye concentration of 20 mg L^{-1}. Very low desorption of dye suggests that chemisorption might be the major mode of dye removal by the adsorbent[23].

Effects of agitation time and adsorbent dose

A series of contact time experiments for adsorption of DR 12B dye were carried out at different initial concentrations (DR 12B 10-50 mg L^{-1}) at 35°C. The equilibrium time for DR 12B was found to be 120 min and 140 min for 10 and 20 mg L^{-1}, respectively and 160 min for the remaining concentrations. The per cent removal decreased with increasing initial dye concentration and the dye adsorption capacity of ZAJHC was increased with an increase in the initial dye concentration. Initial concentration provides an important driving force to overcome all mass transfer resistances of the dye between the aqueous and solid phases. Hence a higher initial concentration of dye will enhance the adsorption process. The equilibrium adsorption capacity of DR 12B with initial dye concentrations at 10 to 50 mg L^{-1} were found to be 10 to 39.31mg g^{-1} (Ref 24). By increasing the adsorbent dose the removal of DR 12B increased to 100% at 150, 200, 250 and 300 mg per 50 mL of ZAJHC for 10-50 mg L^{-1} concentrations of DR 12B, respectively[10].

Adsorption kinetics

A study of adsorption kinetics models correlates the adsorbate uptake rate with the bulk concentration of the adsorbate; these models are important in design and optimization of water/wastewater treatment processes. In order to examine the rate controlling steps, the kinetic data were modelled using Lagergren first order, pseudo-second-order and intraparticle diffusion equations.

First order kinetic model

The Lagergren rate equation is the most widely used adsorption rate equation for the sorption of liquid/solid system based on solid capacity. Adsorption of DR 12B was analyzed using the Lagergren first order rate equation[25]

$$\log(\mathrm{q_e} - \mathrm{q}) = \log \mathrm{q_e} - \frac{k_1 t}{2.303} \qquad \text{...(1)}$$

where q_e and q are the amounts of dye adsorbed (mg g^{-1}) at equilibrium and at time t (min) respectively. k_1 is the Lagergren rate constant of first order adsorption (min^{-1}). Values of the q_e and k_1, respectively, were calculated from the slope and intercept of the plots of *log* $(q_e - q)$ versus t (figure not shown).

The pseudo second order kinetic model can be represented as

$$\frac{t}{q} = \frac{1}{k_2 \, q_e^{\,2}} + \frac{1}{q_e} \qquad \text{... (2)}$$

where k_2 is the equilibrium rate constant of pseudo second order adsorption (g mg^{-1} min^{-1}). Values of k_2 and q_e were calculated from the plots of t/q versus t (figure not shown). The computed results obtained from the first and second order kinetic models along with the experimental q_e values are presented in Table 2. The calculated q_e values of the Lagergren first order kinetics are generally closer to the experimental q_e values compared to the calculated q_e values from second order kinetics for DR 12B. So the adsorption process follows Lagergren first order kinetic model for DR 12B dye[26]. Adsorption of dyes is the rate of the process not depend only on the concentration factor (Pseudo-first order) and the rate of the process depends on both concentration as well as time (Pseudo-second order) [27].

Intrapartical diffusion

An empirically found functional relationship for intrapartical diffusion, common to the most adsorption processes, is that the uptake varies with $t^{1/2}$. According to Weber and Morris[28]

$$q_t = k_{id}\, t^{1/2} \qquad \text{... (3)}$$

where q_t is the amount adsorbed (mg g^{-1}) at time, t (min) and k_{id} (mg g^{-1} $h^{-1/2}$) is the intra-particle diffusion rate constant. All the plots have the same general features: (i) the initial curved portion is attributed to the bulk diffusion effect, (ii) the linear portion to the intraparticle diffusion effect and (iii) the plateau to the equilibrium. The linear portions of the plots do not pass through the origin indicating that intraparticle diffusion is not the only rate controlling step for adsorption process. When adsorbate in solution is mixed with the adsorbent, there occurs transport of the dye into the pores of particles from the solution through the interface between the solution and the adsorbent[29]. According to Eq. 3, the slopes of the linear portions of the plots of q_t vs $t^{1/2}$ (Figure not shown) give the values of k_{id} (Table 2). Values of intercept give an idea about the thickness of boundary layer, i.e., larger the intercept the greater is the boundary layer effect. The linear portions are attributed to the instantaneous utilization of the most readily available adsorbing sites on the adsorbent surface. One could observe that the diffusion in bulk phase to the exterior surface of adsorbent, which started at onset of the process, was the fastest and the second portion of the plot seemed to refer to the diffusion into mesopores. This implied that the intraparticle diffusion of dye molecules into mesopores was the rate-limiting step in the adsorption process onto ZAJHC, particularly over long contact time periods[30].

Table 2 — Comparison of Lagergren first order and second order kinetic data for adsorption of DR 12B onto ZAJHC

Kinetic Model	Conc (mg L^{-1})	q_e exp (mg g^{-1})	k_1 (min^{-1})	q_e cal (mg g^{-1})	R^2
First Order	10	10	0.05	9.81	0.98
	20	19.75	0.02	17.2	0.99
	30	28.81	0.02	27.51	0.99
	40	34.71	0.02	34.41	0.96
	50	39.07	0.02	40.86	0.95
	Conc (mg L^{-1})	q_e exp (mg g^{-1})	K_2 (g mg^{-1} min^{-1})	q_e cal (mg g^{-1})	R^2
Second Order	10	10	0.006	11.45	0.99
	20	19.75	0.002	23.20	0.98
	30	28.81	0.001	34.60	0.98
	40	34.71	0.001	40.98	0.97
	50	39.07	0.001	47.39	0.97
	Conc (mg L^{-1})	q_e exp (mg g^{-1})	k_{id} (mg $g^{-1}h^{-1/2}$)	C	R^2
Intraparticle diffusion	10	10	0.5168	4.775	0.76
	20	19.75	1.3836	4.5967	0.937
	30	28.81	2.2455	2.9367	0.972
	40	34.71	2.7	2.9792	0.983
	50	39.07	3.111	2.7868	0.983

Adsorption Isotherms

Adsorption isotherm is the most important information, which indicates how adsorbate molecules are distributed between the liquid phase and solid phase when the adsorption process reaches equilibrium. This study adopted the Langmuir, Freundlich and D–R isotherms to describe equilibrium adsorption[31].

Langmuir Isotherm

The Langmuir adsorption model[32] is based on the assumption that maximum adsorption corresponds to a saturated monolayer of solute molecules on the adsorbent surface, with no lateral interaction between the adsorbed molecules. The Langmuir adsorption isotherm has been successfully used to explain the adsorption of direct dye from aqueous solutions.

The linear form of Langmuir's isotherm is represented by the equation[33];

$$\frac{C_e}{q_e} = \frac{1}{Q_0 b} + \frac{C_e}{Q_0} \qquad \text{... (4)}$$

where C_e is the equilibrium concentration (mg L^{-1}), q_e is the amount adsorbed at equilibrium (mg g^{-1}) and Q_o and b are Langmuir constants related to adsorption efficiency and energy of adsorption, respectively. The linear plots of C_e/q_e vs C_e suggest the applicability of the Langmuir isotherms

Table 3 — Langmuir, Freundlich and Dubinin- Radushkevich isotherm constants for adsorption of Direct Red 12B

		Langmuir					Freundlich				D-R			
Dyes	Conc mg L^{-1}	Q_0 (mg g^{-1})	B (L mg^{-1})	R^2	R_L	Δq (%)	k_f $mg^{1-1/n}L^{1/n}g^{-1}$	n	R^2	Δq (%)	q_m (mg g^{-1})	β (mol^2J^2 x 10^{-9})	R^2	Δq (%)
DR 12B	10				0.04									
	20				0.02									
	30	39	2.56	0.997	0.01	16.92	23.32	3.87	0.891	18.34	140.51	1	0.915	104.33
	40				0.01									
	50				0.01									

(figure not shown). Values of Q_o and b were determined from slope and intercepts of the plots (Table 3). The values of Q_o and b indicate that the maximum adsorption corresponds to a saturated monolayer of adsorbate molecules on adsorbent surface with constant energy and no transmission of adsorbate in the plane of the adsorbent surface. To confirm the favourability of the adsorption process, the separation factor (R_L) was calculated.

$$R_L = \frac{1}{(1+bC_0)} \quad \text{... (5)}$$

The R_L values obtained were between 0 and 1 (0.04 to 0.01 for DR 12B) (Table 4). This indicates that the adsorption process is favourable[34]. Comparison of Langmuir adsorption capacity by various adsorbent from literature is presented in Table 4.

Table 4 — Comparison of Langmuir constants for adsorption capacity by various adsorbents from literatures

S.No	Adsorbate	Adsorbent	Langmuir isotherm Q_o (mg/g)	Reference
1		Biogas residualslurry	3.46	23
		Banana pith	4.76	23
2		Fe(III)/Cr(III) hydroxide	5.00	35
3		AC/Hazelnut shells	18.24	36
4		AC/Garlic peel	37.96	37
5	Direct Red 12B	Banana pith	5.92	38
6		Rice husk/PVA-alginate immobilised	11.44	39
7		AC/Rice bran/293K	1.29	40
8		AC/Rice bran/303K	1.23	40
9		AC/Rice bran/318K	1.02	40
10		AC/Rice bran/328K	0.99	40
11		ZAJHC	39.00	This work

Freundlich Isotherm

The Freundlich isotherm describes equilibrium on heterogeneous surfaces and hence does not assume monolayer capacity. A linear form of the Freundlich model is represented by the equation[41]:

$$\log q_e = \log k_f + \frac{\log C_e}{n} \quad \text{... (6)}$$

where k_f and n are constants incorporating the factors affecting the adsorption capacity and intensity of adsorption, respectively. Linear plots of *log* q_e vs *log* C_e suggest that the adsorption follows Freundlich isotherm. The values of n ranging from 1.0 to 10.0 indicated a good adsorption process (Table 3).

D-R isotherm

The D-R isotherm is represented as:

$$\ln q_e = \ln q_m - \beta\varepsilon^2 \quad \text{... (7)}$$

where β is a constant related to the mean free energy of adsorption (mol^2 kJ^{-2}), q_m is the theoretical saturation capacity (mg g^{-1}), ε is the polyani potential, and calculated as follows:

$$\varepsilon = RT \ln (1+\frac{1}{C_e}) \quad \text{... (8)}$$

The slope of the plot of *ln* q_e vs ε^2 gives β and the intercept yields the adsorption capacity (figures not shown). The mean free energy of adsorption (E) (kJ mol^{-1}) is calculated from the equation (9):

$$E = \frac{1}{\sqrt{2\beta}} \quad \text{... (9)}$$

If the value of E is less than 8 kJ mol^{-1}, the adsorption follows physical sorption. If the value of E is between 8 and 16 kJ mol^{-1}, the adsorption follows ion exchange. If the E value is above 40 kJ mol^{-1} the adsorption follows chemisorption. Values of

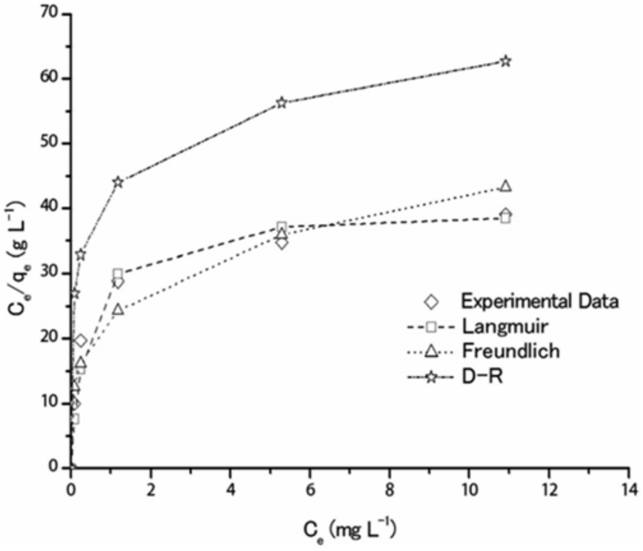

Fig. 4 — Comparison of Langmuir, Freundlich and D-R isotherms for adsorption of DR 12B

E obtained for DR 12B is 22.37 kJ mol^{-1}. Hence adsorption involved seems to be chemisorption[42]. Figure 4 represent different adsorption isotherms along with the experimental data for adsorption DR 12B. In order to compare the validity of isotherm equations, a normalized deviation, Δq (%) was calculated using the equation (10):

$$\Delta q\,(\%) = 100 \times \sqrt{\frac{\sum\left[\left(\frac{q_e^{\exp} - q_e^{cal}}{q_e^{\exp}}\right)\right]^2}{(n-1)}} \qquad \text{... (10)}$$

where superscripts '*exp*' and '*cal*' are the experimental and calculated values, respectively, and '*n*' is the number of measurements[43]. Lowest Δq (%) values obtained from the isotherm models indicate highest fitting with the adsorption data. In the present study the Δq (%) values obtained for DR 12B is in the order: Langmuir < Freundlich < D-R (Table 3). Hence Langmuir isotherm fits most with the equilibrium adsorption data for DR 12B. Adsorption capacity values from Langmuir [Q_o] and Freundlich [k_f] isotherms for DR 12B are found to be less, which is due to the bulk structure of DR 12B (higher molecular weight) and also contains two sulphonate groups.

Effect of temperature on adsorption of DR 12B onto ZAJHC

The adsorption studies were carried out at four different temperatures 308, 313, 323and 333 K. The adsorption capacity increased with the increasing temperature, indicating that the adsorption was an endothermic process. This may be a result of increase in the mobility of the dye with increasing temperature and increasing temperature may also produce a swelling effect within the internal structure of the adsorbents enabling large dye to penetrate further. Similar trends were also observed by other researchers for aqueous phase adsorption[44].

Table 5 — Thermodynamic parameters for the adsorption of DR 12B onto ZAJHC

T (K)	K_c	ΔG (KJmol^{-1})	ΔH (KJmol^{-1})	ΔS (J mol^{-1} K^{-1})
308	24.25	-8.17		
313	199	-13.77		
323	184.19	-14.01	3.08	66.77
333	624	-17.82		

Thermodynamic parameters such as change in free energy (ΔG^o), enthalpy (ΔH^o) and entropy (ΔS^o) were calculated using the equations (11 & 12):

$$\Delta G^0 = 2.303\,RT\log K \qquad \text{... (11)}$$

$$\log \mathrm{K} = \frac{\Delta \mathrm{S}^o}{2.303\mathrm{R}} - \frac{\Delta H^o}{2.303RT} \qquad \text{... (12)}$$

where K (=b) is the adsorption equilibrium constant, R is the gas constant (8.314 J K^{-1} mol^{-1}), T is the absolute temperature (K), respectively. ΔH^o and ΔS^o were obtained from Eq. (12). The positive value of ΔH^o indicated that the process was endothermic in nature (Table 5). The negative values of ΔG^o indicated spontaneous nature of the adsorption of DR 12B onto the adsorbent[45].

FTIR Study

Nature of the chemical bonding and functional groups of the DR 12B loaded ZAJHC was observed from FTIR spectroscopy. The FTIR spectra were recorded on pellets obtained by pressing mixture of 1 mg of the ZAJHC and 100 mg of dried KBr under pressure. Figures 5(a) and (b) show FTIR spectra of ZAJHC and DR 12B loaded ZAJHC observed in the range of 450 to 4500 cm^{-1}. The FTIR spectrum of the ZAJHC characteristics peaks at 3450 cm^{-1} (OH group), bands at 2923 and 2857 cm^{-1} (asymmetric and symmetric vibration of C-H groups), and 1630 cm^{-1} (C=O group) were observed[46].

For DR 12B loaded ZAJHC shows characteristic at 1078, 1556, 1784, 2825, 3049 and 3722 cm^{-1}. The absorption peak at 1150-1000 cm^{-1} corresponds to the stretching vibration of C-O group. The peaks at 1078 and 1784 cm^{-1} represent the C-O symmetric and C-O stretching vibrations, respectively. The strong and sharp peak at 1556 cm^{-1} is related to stretching

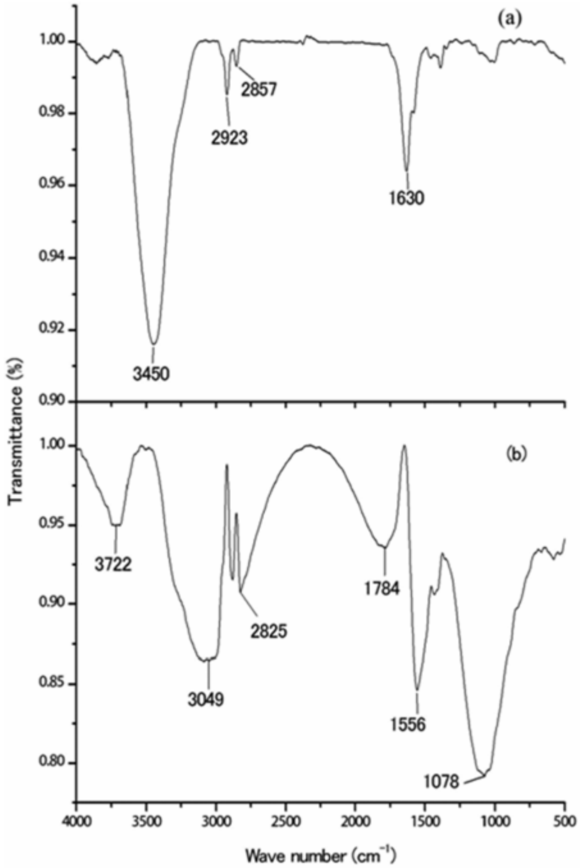

Fig. 5 — FT-IR spectra of ZAJHC before (a) and after adsorption of DR 12B (b)

vibration of secondary amine group. The CH_2 asymmetric and symmetric stretching vibration in the structure of the cellulose, hemicellulose and lignin were ascribed to 2825 cm^{-1}. The characteristic peaks observed at 3049 and 3722 cm^{-1} denote the vibration of O-H functional group[47].

Conclusion

Batch adsorption studies were conducted to evaluate the effect of various parameters such as initial dye concentration, *p*H, agitation time, adsorbent dosage and temperature on the removal of DR 12B by ZAJHC. The *p*H of the dye solution strongly affected the chemistry of both the dye molecules and adsorbent in aqueous solutions. Maximum removal was found to be at *p*H 2.0. The adsorption followed Lagergren first order kinetics. The adsorption equilibrium data were treated by Langmuir, Freundlich and D-R isotherm equations. The experimental data yielded excellent fit with Langmuir isotherm equation. Different thermodynamic parameters viz., changes in standard free energy, enthalpy and entropy were evaluated and it was found that the reaction was spontaneous and endothermic in nature. The results showed that the adsorbent can be used as a low-cost material for the removal of DR 12B from aqueous solutions.

Acknowledgement

Authors are grateful to Dr. K. Kadirvelu (Scientist), DRDO-BU Centre for Life Sciences, Bharathiar University Campus for providing SEM and FTIR Spectra for the samples.

References

1 Orfao J J M, Silva A I M, Pereira J C V, Barata S A, Fonseca I M, Faria P C C & Pereira M F R, *J Colloid and Inter Sci*, 296 (2006) 480.

2 Amin N K, *Desalination*, 223 (2008) 152.

3 Calvete T, Lima E C, Cardoso N F, Vaghetti J C P, Dias S L P & Pavan F A, *J Environ Manag*, 91 (8) (2010) 1695.

4 Pereira L, Pereira R, Pereira M F R, van der Zee F P, Cervantes F J & Alves M M, *J Hazard Mater*, 183 (2010) 931.

5 Fu J, Xu Z, Li Q S, Chen S, An S Q, Zeng Q F & Zhu H L, *J Environ Sci*, 22(4) (2010) 512.

6 Sinha K, Saha P D & Datta S, *Indus Crops and Prod*, 37 (2012) 408.

7 Dave P N, Kaur S & Khosla E, *Indian J Chem Technol*, 18 (2011) 53.

8 Lee J W, Choi S P, Thiruvenkatachari R, Shim W G & Moon H, *Dyes and Pigments*, 69 (2006) 196.

9 Bazrafshan E, Zarei A A, Nadi H & Zazouli M A, *Indian J Chem Technol*, 21 (2014) 105.

10 Namasivayam C & Kavitha D, *Dyes Pigments*, 54 (2002) 47.

11 Ponnusami V, Krithika V, Madhuram R & Srivastava S N, *J Hazard Mater*, 142 (1-2) (2007) 397.

12 Ramakrishnan K & Namasivayam C, *J Environ Engg Manag*, 19 (3) (2009) 173.

13 Baseri J R, Palanisamy P N & Kumar P S, *Indian J Chem Technol*, 19 (2012) 311.

14 Karthick K, Dinesh C & Namasivayam C, *Sustain Environ Res*, 24 (2) (2014) 139.

15 Namasivayam C & Sangeetha D, *J Hazard Mater, B* 135 (2006) 449.

16 Sabio M M & Reinose F R, *Colloid Surf A: Physicochem Engg Aspect*, 241 (2004) 15.

17 Farouqui F I, Sheikh M R K, Hossain M I & Saha S K, *Indian J Chem Technol*, 4 (4) (1997) 185.

18 Vandevivere P C , Bianchi R & Verstraete W, *J Chem Technol Biotechnol*, 72 (4) (1998) 289.

19 Annadurai G, Juang R S & Lee D J, *J Hazard Mater B*, 92 (2002) 263.

20 Tunc O, Tanaci H & Aksu Z, *J Hazard Mater*, 163 (1) (2009) 187.

21 Ozcan A S & Ozcan A, *J Colloid Inter Sci*, 276 (2004) 39.

22 Chen M, Ding W, Wang J & Diao G, *Indus Engg Chem Res*, 52 (2013) 2403.

23 Namasivayam C & Sumithra S, *J Environ Manag*, 74 (2005) 207.

24 Sureshkumar M V & Namasivayam C, *Colloids Surf A: Physicochem Engg Asp*, 317 (2008) 277.

25 Lagergren S, *Handlingar*, 24 (4) (1898) 1.

26 Namasivayam C, Prabha D & Kumutha M, *Biores Technol*, 64 (1998) 77.

27 Kumar M & Tamilarasan R, *J Mat Environ Sci*, 5 (2) (2014) 510.

28 Weber W J & Morris J C, *J San Engg Div*, 89 (2) (1963) 31.

29 Cheung W H, Szeto Y S & McKay G, *Biores Technol*, 98 (2007) 2897.

30 Qin Q, Ma J & Liu K, *J Hazard Mater*, 162 (2009) 133.

31 Kuo C Y, Wu C H & Wu J Y, *J Colloid Inter Sci*, 327 (2008) 308.

32 Hameed B H, Mahmoud D K & Ahmad A L, *J Hazard Mater*, 158 (2008) 65.

33 Namasivayam C & Sureshkumar M V, *J Appl Polym Sci*, 100 (2) (2006) 1538.

34 Jagadeesh Kumar A & Namasivayam C, *Sustain Environ Res*, 24 (1) (2014) 73.

35 Gupta V K & Suhas, *J Environ Manag*, 90 (2009) 2313.

36 Fathi M R & Asfaram A, *J Chem Health Risks*, 1 (2) (2011) 1.

37 Asfaram A, Fathi M R, Khodadoust S & Naraki M, *Spectrochimica Acta Part A: Mol Biomol Spectroscopy*, 127 (2014) 415.

38 Soltani R D C, Khataee A & Koolivand A, *Environ Prog & Sustainable Energy*, (2015) 1.

39 Safa Y, Bhatti H N, Bhatti I A & Asgher M, *The Canadian J Chem Engg*, 89 (2011) 1554.

40 Sankar M, Sekaran G, Sadulla S & Ramasami T, *J Chem Technol Biotechnol*, 74 (1999) 337.

41 Demirbas E & Nas M Z, *Desalination*, 243 (1–3) (2009) 8.

42 Abasi C Y, Abia A A & Igwe J C, *Environ Res J*, 5 (3) (2011) 104.

43 Subha R & Namasivayam C, *Bioremed J*, 14 (1) (2010) 1.

44 Asfour H M, Nassar M M, Fadali O A & El-Geundi M S, *J Chem Technol Biotechnol A*, 35 (1985) 28.

45 Hamadi N K, Chen X D, Farid M M & Lu M G Q, *Chem Engg J*, 84 (2001) 95.

46 Ursescu M, Maluţan T & Ciovica S, *Eur J Sci Theol*, 5 (3) (2009) 71.

47 Silva S M L, Braga C R C, Fook M V L, Raposo C M O, Carvalho L H & Canedo E L, *Infrared Spectroscopy - Materials Science, Engineering and Technology* (InTech, Europe), 2012, 51.